

Error analysis based on inverse modified differential equations for discovery of dynamics using linear multistep methods and deep learning

Aiqing Zhu¹, Sidi Wu¹, and Yifa Tang^{1*}

¹LSEC, ICMSEC, Academy of Mathematics and Systems Science, Chinese Academy of Sciences, Beijing 100190, China

*Email address: tyf@lsec.cc.ac.cn

Abstract

Along with the practical success of the discovery of dynamics using deep learning, the theoretical analysis of this approach has attracted increasing attention. Prior works have established the grid error estimation with auxiliary conditions for the discovery of dynamics via linear multistep methods and deep learning. And we extend the existing error analysis in this work. We first introduce the inverse modified differential equations (IMDE) of linear multistep methods and show that the learning model returns a close approximation of the IMDE. Based on the IMDE, we prove that the error between the discovered system and the target dynamical system is bounded by the sum of the LMM discretization error and the learning loss. Several numerical experiments are performed to verify the theoretical analysis.

Key words. learning dynamics, data-driven discovery, linear multistep methods, deep learning, backward error analysis.

1 Introduction

Discovery of hidden dynamical systems from observed data is a significant and challenging task across diverse scientific fields [7, 8, 49], and also plays an important role in various applications of machine learning such as robotic manipulation [25] and autonomous driving [36]. Besides some popular approaches such as symbolic regression [4, 49], sparse regression [8, 47], Gaussian process [42, 34] and Koopman theory [6], numerous approaches leverage deep learning to discover mathematical models from data. We refer the reader to [15] for a comprehensive overview of techniques for the discovery of dynamics. There were multiple pioneering efforts using neural networks to model continuous time-series data in the 1990s [1, 18, 45, 46]. In recent years, a growing number of models combining numerical integrators and neural networks have been developed and applied to learn hidden dynamics expressed by differential equations [11, 27, 35, 40, 43]. In addition, such learning models are further extended to incorporate the physics inductive bias of the underlying problems [3, 5, 19, 28, 39, 54, 56, 57].

With the satisfactory progress of the discovery using deep learning, our theoretical understanding of it is also being developed [15, 32, 58]. This work focuses on the discovery of dynamics using linear multistep methods (LMMs) and deep learning, coined LMNets [15, 32, 43, 51], which is essentially an inverse process of identifying the unknown governing function f of a dynamical system using provided information of the flow map on given phase points. And we aim to extend the prior existing error estimations for such a learning model in [15, 32] from a new perspective.

To begin with, we briefly review the data-driven discovery models LMNets following [15, 32, 43]. Suppose the vector-valued functions $y(t) : \mathbb{R} \rightarrow \mathbb{R}^D$ and $f(y) : \mathbb{R}^D \rightarrow \mathbb{R}^D$ obey the differential equation

$$\frac{d}{dt}y(t) = f(y(t)) \quad (1)$$

but are both unknown. The objective is to find a closed-form expression for the unknown target governing function f with given $y_n = y(nh)$ for $n = 0, \dots, N$. By applying an LMM, we can build the discrete relation between the states y_n and the approximations $f_n \approx f(y_n)$ [15, 32, 43], i.e.,

$$\sum_{m=0}^M \alpha_m y_{n+m} - h \sum_{m=0}^M \beta_m f_{n+m} = 0, \quad n = 0, \dots, N - M. \quad (2)$$

To obtain the closed-form expressions, we employ a neural network f_θ to approximate f . The parameter of f_θ can be obtained by optimizing the training loss obtained by replacing each f_n in (2) with $f_\theta(y_n)$,

$$J_h = \frac{1}{N - M + 1} \sum_{n=0}^{N-M} \left\| \sum_{m=0}^M h^{-1} \alpha_m y_{n+m} - \sum_{m=0}^M \beta_m f_\theta(y_{n+m}) \right\|_2^2. \quad (3)$$

After optimization, the unknown f is recovered with an explicit expression, and we can predict the dynamics on nearby data via solving (1) by means of the generalization of deep learning.

Although the f_n might not be all involved in (2), we typically have more unknowns than we have equations. Thus the linear system (2) has infinitely many solutions and J_h admits infinitely many global minimizers which lead to near-zero loss but might totally different from the target governing function. In [32], the auxiliary conditions are proposed to ensure the uniqueness, and a framework based on refined notions is established for the rigorous convergence and stability analysis. Until recently the best error estimation was due to Du et al. [15]. By introducing an augmented loss function based on the auxiliary conditions, they prove that the grid error of the global minimizer is bounded by the sum of the discretization error and the approximation error, yielding that LMNets are able to have high error orders.

However, prior existing analysis [15, 32] concentrate on training networks with auxiliary conditions, and only quantify the error evaluated at the given sample locations. In practice, the use of deep learning approach introduces further implicit regularization. Du et al. [15] numerically find that LMNets without the auxiliary conditions still perform well as long as the time step size is sufficiently small. They conjecture that this is due to the implicit regularization that the gradient descent tends to find a very smooth function among all global minimizers. In addition, we typically need to forecast the future behavior of the same dynamics or predict other dynamics, and are thus inevitably faced with the generalization error. Whereas numerical results show excellent generalization performance [15, 43], the error out of sample locations needs further precise quantification.

We partially solved these open questions, i.e., quantifying the error out of sample locations without the auxiliary conditions. Inspired by the implicit regularization discussed in [15], we assume that the target governing function f and the learned neural network f_θ are analytic and bounded to further quantify the smoothness. Such analyticity hypotheses indicate the boundedness of derivatives of f and f_θ , and exclude the solutions with high-frequencies due to Cauchy’s estimate in several variables, allowing us to perform numerical analysis without auxiliary conditions. In addition, we use the learning loss on the complex neighborhood of the given point as the upper bound of the error. This makes it possible to estimate the error without taking into account the sample locations.

The major ingredients are the formal analysis [16, 17] as well as the inverse modified differential equations (IMDE) proposed in our conference paper [58]. Following the framework introduced in [32], we first find a perturbed differential equation, i.e., the IMDE, such that it satisfies the multistep relation (2) formally. The explicit recursion formula of IMDE is given by means of the Lie derivatives and the multistep formula. In addition, inspired by the rigorous estimates of modified differential equations [2, 21, 20, 44], we truncate IMDE and prove that the difference between the learned network and the truncated IMDE is bounded by the learning loss and a discrepancy that can be made exponentially small, which implies the uniqueness of the solution of the learning task (3) in some sense. Our proof is completely different from that of previous work [58], and yields sharper estimates. Next, via investigating IMDE, we show that the error between the learned network and the target governing function is bounded by the sum of the LMM discretization error $\mathcal{O}(h^p)$ and the learning loss when using a p -th order LMM with step size h . It is remarked that our conclusions do not depend on auxiliary conditions, and hold for any weakly stable and consistent LMM.

This paper is organized as follows. In Section 2, we briefly provide some necessary notations and preliminaries. In Section 3, we give the explicit recursion formula of the IMDE of LMMs. In Section 4, we study the difference between the target governing function and the suitably truncated IMDE, and present the main results (Theorem 2) and their proofs in detail. In Section 5, several numerical results are provided to verify the theoretical findings. Finally, we give a brief summary and several comments on the future work in Section 6.

2 Preliminaries

2.1 Dynamical systems

Without loss of generality, the attention in this paper will be addressed to autonomous systems of first-order ordinary differential equations

$$\frac{d}{dt}y(t) = f(y(t)), \quad y(0) = x, \quad (4)$$

where $y(t) \in \mathbb{R}^D$ and $f : \mathbb{R}^D \rightarrow \mathbb{R}^D$ is smooth. The initial value is denoted as x in this paper. A non-autonomous system $\frac{d}{dt}y(t) = f(t, y(t), p)$ with parameter p can be brought into this form by appending the equations $\frac{d}{dt}t = 1$ and $\frac{d}{dt}p = 0$. For fixed t , $y(t)$ can be regarded as a function of its initial value x . We denote

$$\phi_t(x) := y(t) = x + \int_0^t f(y(\tau))d\tau,$$

which is known as the time- t flow map of dynamical system (4). In the following sections, we will add the subscript f and denote ϕ_t as $\phi_{t,f}$ to emphasize specific differential equation.

2.2 Linear multistep methods

For first order differential equations (4), linear multistep methods (LMMs) are defined by the formula

$$\sum_{m=0}^M \alpha_m y_m - h \sum_{m=0}^M \beta_m f(y_m) = 0, \quad (5)$$

where α_m, β_m are specified coefficients, $\alpha_M \neq 0$ and $|\alpha_0| + |\beta_0| > 0$. When applying an LMM to solve a differential equation (4), a starting method for initial M values y_1, \dots, y_{M-1} must be chosen and the approximations y_n for $n \geq M$ can then be computed recursively. The method (5) is called explicit if $\beta_M = 0$, otherwise it is implicit and y_n for $n \geq M$ can be computed iteratively by fixed-point iteration or Newton-Raphson iteration. Next, we present some basic notations and concepts following [23, 24].

Weak stability. An LMM is weakly stable if

$$\sum_{m=0}^M m \cdot \alpha_m \neq 0. \quad (6)$$

Consistency. An LMM is consistent if

$$\sum_{m=0}^M \alpha_m = 0, \text{ and } \sum_{m=0}^M m \cdot \alpha_m = \sum_{m=0}^M \beta_m. \quad (7)$$

Order. An LMM is of order p ($p \geq 1$) if

$$\sum_{m=0}^M \alpha_m = 0, \text{ and } \sum_{m=0}^M \frac{m^{k+1}}{(k+1)!} \cdot \alpha_m = \sum_{m=0}^M \frac{m^k}{k!} \cdot \beta_m \text{ for } k = 0, 1, \dots, p-1. \quad (8)$$

In this paper, we concentrate on weakly stable and consistent linear multistep methods, where $\sum_{m=0}^M \beta_m \neq 0$ due to the weak stability condition (6) and the consistency condition (7). Thus we assume $\sum_{m=0}^M \beta_m = 1$ without loss of generality.

2.3 Neural networks

We briefly describe the setting of the supervised learning problem using neural networks in this subsection. Let \mathcal{M} denote the hypothesis space consisting of neural networks. In this paper, we will focus on a widely used architecture known as fully connected neural networks (FNNs). Mathematically speaking, an FNN, denoted as $f_\theta(x)$, is the composition of linear layers and activation layers, i.e.,

$$f_\theta(x) = W_{L+1} h_L \circ h_{L-1} \circ \dots \circ h_1(x) + b_{L+1},$$

where

$$h_l(z_l) = \sigma(W_l z_l + b_l), \quad W_l \in \mathbb{R}^{d_l \times d_{l-1}}, b_l \in \mathbb{R}^{d_l} \text{ for } l = 1, \dots, L+1.$$

The number L is the total number of layers, $\theta = \{W_l, b_l\}_{l=1}^{L+1}$ are trainable parameters, and $\sigma : \mathbb{R} \rightarrow \mathbb{R}$ is a predetermined activation function and is applied element-wise to a vector. Popular examples include the rectified linear unit (ReLU) $\text{ReLU}(z) = \max(0, z)$, the sigmoid $\text{Sig}(z) = 1/(1 + e^{-z})$ and $\text{tanh}(z)$.

Let $x \in \mathcal{X}$ be inputs, $f(x)$ be the corresponding targets, and $l(\cdot, \cdot)$ be a loss function¹, the goal of supervised learning is typically framed as an optimization problem of the form

$$\inf_{f_\theta \in \mathcal{M}} \mathcal{R}(f_\theta), \text{ where } \mathcal{R}(f_\theta) = \int_{\mathcal{X}} l(f_\theta(x), f(x)) dP(x).$$

The objective function $\mathcal{R}(f_\theta)$ is known as the expected loss of a network f_θ . In practice, the probability measure P is unknown. And thus we sample training data $\{(x_n, f(x_n))\}_{n=1}^N$ and set P to be the empirical measure, yielding the empirical risk optimization problem

$$\inf_{f_\theta \in \mathcal{M}} \mathcal{R}_S(f_\theta), \text{ where } \mathcal{R}_S(f_\theta) = \frac{1}{N} \sum_{n=1}^N l(f_\theta(x_n), f(x_n)). \quad (9)$$

The objective function $\mathcal{R}_S(f_\theta)$ is called the training loss since it is the loss function evaluated the training data. FNN can approximate essentially any function if its size is sufficiently large [12, 14, 26, 38], and the optimization technique in deep learning can effectively reduce the above training loss (9) [30, 55]. Although non-vacuous generalization bounds remain elusive, in practice, neural network models have better generalization, i.e., small loss on unknown data, and we can directly use the test loss evaluated on test data to measure the learning performance [29, 31].

The use of over-parameterized FNN typically leads to non-uniqueness of global minimizers, but there is further implicit regularization to prevent over-fitting. It has been shown that training neural networks using gradient descent learns the low-frequency modes first and then fits the high-frequency modes to eliminate the training loss [10, 41, 52, 53]. This implicit bias indicates that networks trained by gradient descent prioritize learning smooth functions with low frequencies among all solutions with near-zero training loss. Such implicit regularization was first discussed in [15] for the discovery of dynamics, and also motivates us to make the analyticity hypotheses in this work, which will be documented in detail later.

2.4 Discovery of dynamics using LMMs

The optimization problem (3) is specific to the discovery on single trajectory. More generally, we consider training data given as

$$\mathcal{T}_{train} = \left\{ (x_n, \phi_{h,f}(x_n), \dots, \phi_{Mh,f}(x_n)) \right\}_{n=1}^N.$$

If the states at equidistant time steps of some trajectories are given, we can group them in pairs to get the above form. Specifically, suppose we are given a dataset $\{\phi_{nh,f}(\tilde{x}_{n'})\}_{n=0, \dots, N; n'=1, \dots, N'}$ with initial points set $\{\tilde{x}_{n'}\}_{n'=1, \dots, N'}$, we can denote them as

$$\left\{ (x_n, \phi_{h,f}(x_n), \dots, \phi_{Mh,f}(x_n)) \mid x_n = \phi_{nh,f}(\tilde{x}_{n'}) \right\}_{n=0, \dots, N-M; n'=1, \dots, N'}.$$

¹A common choice for regression problems is the square loss, $l(y, \hat{y}) = \|y - \hat{y}\|_2^2$.

Then the training loss (3) of the dynamics discovery can be rewritten as

$$J_h = \frac{1}{N} \sum_{n=0}^N \left\| \sum_{m=0}^M h^{-1} \alpha_m \phi_{mh,f}(x_n) - \sum_{m=0}^M \beta_m f_\theta(\phi_{mh,f}(x_n)) \right\|_2^2, \quad (10)$$

which is formally close to (9) except for the specially designed loss function. Similar to the standard supervised learning problem, the gradient-based optimization techniques in deep learning are able to not only minimize the training loss, but also achieve small loss on unknown data. After training, the returned network f_θ serves as an approximation of the target governing function f in a closed-form.

3 Inverse modified differential equations of LMMs

To begin with, we seek a perturbed differential equation

$$\frac{d}{dt} \tilde{y}(t) = f_h(\tilde{y}(t)) = f_0(\tilde{y}) + h f_1(\tilde{y}) + h^2 f_2(\tilde{y}) + \dots, \quad (11)$$

such that formally

$$\sum_{m=0}^M \alpha_m \phi_{mh,f}(x) = h \sum_{m=0}^M \beta_m f_h(\phi_{mh,f}(x)), \quad (12)$$

where identity is understood in the sense of the formal power series in h without taking care of convergence issues. In this paper, we name the perturbed equation (11) as inverse modified differential equation (IMDE), since modified differential equation [16, 17, 20, 23] for forward problem is also a perturbed differential equation $\frac{d}{dt} \hat{y}(t) = \hat{f}_h(\hat{y}(t))$ satisfying an analogous relationship

$$\sum_{m=0}^M \alpha_m \phi_{mh,\hat{f}_h}(x) = h \sum_{m=0}^M \beta_m \hat{f}_h(\phi_{mh,\hat{f}_h}(x)).$$

To this end, we first briefly review Lie derivatives following [23]. Given (4), Lie derivative \mathbf{D} is the differential operator defined as:

$$\mathbf{D}g(y) = g'(y)f(y), \text{ for } g : \mathbb{R}^D \rightarrow \mathbb{R}^D.$$

Therefore, using the chain rule we derive that

$$\frac{d}{dt} g(\phi_{t,f}(x)) = (\mathbf{D}g)(\phi_{t,f}(x))$$

and thus obtain the Taylor series of $g(\phi_{t,f}(x))$ developed at $t = 0$:

$$g(\phi_{t,f}(x)) = \sum_{k=0}^{\infty} \frac{t^k}{k!} (\mathbf{D}^k g)(x). \quad (13)$$

In particular, by setting $g(y) = I_D(y) = y$, the identity map, we obtain the Taylor series of the exact solution $\phi_{t,f}$ itself, i.e.,

$$\begin{aligned}\phi_{t,f}(x) &= \sum_{k=0}^{\infty} \frac{t^k}{k!} (\mathbf{D}^k I_D)(x) \\ &= x + tf(x) + \frac{t^2}{2} f'f(x) + \frac{t^3}{6} (f''(f, f)(x) + f'f'f(x)) + \dots\end{aligned}\tag{14}$$

Here, the notation $f'(x)$ is a linear map (the Jacobian), the second order derivative $f''(x)$ is a symmetric bilinear map and similarly for higher order derivatives described as tensors.

Now we are able to present the general formula of the IMDE (11) in a recursive manner.

Theorem 1. *Consider a weakly stable and consistent LMM (5), there exist unique h -independent functions f_k such that for any truncation index K , the truncated IMDE $f_h^K = \sum_{k=0}^K h^k f_k$ satisfies*

$$\sum_{m=0}^M \alpha_m \phi_{mh,f}(x) = h \sum_{m=0}^M \beta_m f_h^K(\phi_{mh,f}(x)) + \mathcal{O}(h^{K+2}).\tag{15}$$

In particular, for $k \geq 0$, the functions f_k are given as

$$f_k(y) = \sum_{m=0}^M \alpha_m \frac{m^{k+1}}{(k+1)!} (\mathbf{D}^k f)(y) - \sum_{m=0}^M \beta_m \sum_{j=1}^k \frac{m^j}{j!} (\mathbf{D}^j f_{k-j})(y).\tag{16}$$

Proof. The approach for computation of f_h is presented in two steps. To begin with, by using the formula (14), the left of (15) can be expanded as

$$\begin{aligned}\sum_{m=0}^M \alpha_m \phi_{mh,f}(x) &= \sum_{m=0}^M \alpha_m \sum_{k=0}^{\infty} \frac{(mh)^k}{k!} (\mathbf{D}^k I_D)(x) \\ &= \sum_{k=0}^{\infty} h^k \left[\sum_{m=0}^M \alpha_m \frac{m^k}{k!} (\mathbf{D}^k I_D)(x) \right].\end{aligned}\tag{17}$$

Subsequently, using (13) with setting $t = mh$ and $g(y) = f_h(y)$, we obtain that

$$h \sum_{m=0}^M \beta_m f_h(\phi_{mh,f}(x)) = h \sum_{m=0}^M \beta_m \sum_{j=0}^{\infty} \frac{(mh)^j}{j!} \sum_{i=0}^{\infty} h^i (\mathbf{D}^j f_i)(x).$$

By interchanging the summation order, we deduce that

$$\begin{aligned}h \sum_{m=0}^M \beta_m f_h(\phi_{mh,f}(x)) &= h \sum_{m=0}^M \beta_m \sum_{k=0}^{\infty} h^k \sum_{j=0}^k \frac{m^j}{j!} (\mathbf{D}^j f_{k-j})(x) \\ &= \sum_{k=0}^{\infty} h^{k+1} \sum_{m=0}^M \beta_m \left[f_k(x) + \sum_{j=1}^k \frac{m^j}{j!} (\mathbf{D}^j f_{k-j})(x) \right].\end{aligned}\tag{18}$$

Comparing coefficients of h^k in (17) and (18) for $k = 0, 1, 2, \dots$ yields

$$\sum_{m=0}^M \alpha_m = 0,$$

the consistency condition, and

$$\sum_{m=0}^M \beta_m \left[f_k(x) + \sum_{j=1}^k \frac{m^j}{j!} (\mathbf{D}^j f_{k-j})(x) \right] = \sum_{m=0}^M \alpha_m \frac{m^{k+1}}{(k+1)!} (\mathbf{D}^{k+1} I_D)(x).$$

Therefore, we conclude that

$$f_k(y) = \sum_{m=0}^M \alpha_m \frac{m^{k+1}}{(k+1)!} (\mathbf{D}^k f)(y) - \sum_{m=0}^M \beta_m \sum_{j=1}^k \frac{m^j}{j!} (\mathbf{D}^j f_{k-j})(y),$$

which uniquely defines the functions f_k in a recursive manner. Here, we have used the fact that $\sum_{m=0}^M \beta_m = 1$ and $\mathbf{D}^{k+1} I_D = \mathbf{D}^k f$. \square

As a direct consequence of the order condition (8) and the recursion formula (16), we have the following corollary.

Corollary 1. *If the LMM is of order p , then, its IMDE obeys*

$$\frac{d}{dt} \tilde{y} = f_h(\tilde{y}) = f(\tilde{y}) + h^p f_p(\tilde{y}) + \dots,$$

where

$$f_p(y) = \left[\sum_{m=0}^M \frac{m^{p+1}}{(p+1)!} \cdot \alpha_m - \sum_{m=0}^M \frac{m^p}{p!} \cdot \beta_m \right] (\mathbf{D}^p f)(y).$$

4 Error analysis

With the correspondence between the definition of IMDE (12) and the LMM loss (10), we are now ready to show that training LMNets returns a close approximation of the truncated IMDE, and thereby formulate the error representation results. Throughout this section we assume that the employed LMM is weakly stable, consistent, and $\sum_{m=0}^M \beta_m = 1$.

4.1 Main results

Let $\mathcal{B}(x, r) \subset \mathbb{C}^D$ be the complex ball of radius $r > 0$ centered at $x \in \mathbb{C}^D$. For a compact subset $\Omega \subset \mathbb{C}^D$, denote its complex neighborhood as

$$\mathcal{B}(\Omega, r) = \bigcup_{x \in \Omega} \mathcal{B}(x, r).$$

We will work with l_∞ -norm on \mathbb{C}^D and denote $\|\cdot\| = \|\cdot\|_\infty$. For an analytic vector field g , we define

$$\|g\|_\Omega = \sup_{x \in \Omega} \|g(x)\|.$$

Then, the main results are given as follows.

Theorem 2. For $x \in \mathbb{R}^D$ and $r_1, r_2 > 0$, suppose the target governing function f is analytic in $\mathcal{B}(x, r_1 + r_2)$, and the learned vector field f_θ is analytic in $\mathcal{B}(x, r_1)$. Suppose $\|f\|_{\mathcal{B}(x, r_1 + r_2)} \leq b_2$ and $\|f\|_{\mathcal{B}(x, r_1)}, \|f_\theta\|_{\mathcal{B}(x, r_1)} \leq b_1 \leq b_2$. For a given LMM of order p with coefficients α_m, β_m , we denote

$$\mathcal{L} = \left\| \sum_{m=0}^M h^{-1} \alpha_m \phi_{mh, f}(\cdot) - \sum_{m=0}^M \beta_m f_\theta(\phi_{mh, f}(\cdot)) \right\|_{\mathcal{B}(x, r)}.$$

Then, there exists a uniquely defined vector field, i.e., the truncated IMDE f_h^K , such that, if $0 < h < h_0$,

$$\begin{aligned} \|f_\theta(x) - f_h^K(x)\| &\leq c_1 b_2 \cdot e^{-\gamma/h} + \frac{\mathcal{L}}{1 - e^{-1}}, \\ \|f_\theta(x) - f(x)\| &\leq c_2 b_2 \cdot h^p + \frac{\mathcal{L}}{1 - e^{-1}}, \end{aligned}$$

where integer $K = K(h)$ and constants γ, h_0, c_1, c_2 depend on $r_1/b_1, r_2/b_2$ and the coefficients α_m, β_m of the LMM.

Here, we call \mathcal{L} the learning loss, since it is the loss function maximized over the neighborhood of the given state and indicates the learning performance of the learned model. The IMDE is inaccessible in practice due to the unknown of the target governing function. However, besides allowing us to formulate the error estimation, it implies the uniqueness of the solution of the learning task (10) in some sense. Under our hypotheses, if training finds a neural network with perfect performance (zero loss), then the difference between the learned network and the truncated IMDE is exponentially small.

In contrast to the idea of introducing auxiliary conditions [15, 32], we use the analyticity hypotheses to ensure the uniqueness of the solution in the function space. We next illustrate this by the following two learning tasks.

Example 1. Consider learning the differential equation

$$\frac{d}{dt}p = 1, \quad \frac{d}{dt}q = \sin \frac{2\lambda\pi}{h} p,$$

with parameter $\lambda \in \mathbb{Z}$ and initial value $(p(0), q(0)) = (p_0, q_0)$. The exact solution is given as

$$p(t) = p_0 + t, \quad q(t) = q_0 - \frac{h}{2\lambda\pi} \left(\cos \frac{2\lambda\pi}{h} (p_0 + t) - \cos \frac{2\lambda\pi}{h} p_0 \right).$$

Taking $t = h$, we have that

$$p(h) = p_0 + h, \quad q(h) = q_0.$$

Same states but different parameter λ indicate the non-uniqueness of the ODE interpretation of the training data.

Example 2. Consider learning the linear equation

$$\frac{d}{dt}p = -1, \quad p(t) = p(0) - t,$$

by using AB schemes with $M = 2$

$$y_2 - y_1 = \frac{3h}{2}f(y_1) - \frac{h}{2}f(y_0),$$

we have

$$p(2h) - p(h) = \frac{3h}{2}f_\lambda(p(h)) - \frac{h}{2}f_\lambda(p(0)), \text{ where } f_\lambda = 1 + \lambda e^{x \ln 3/h},$$

which indicates the non-uniqueness of solutions leading to zero loss.

The analyticity hypotheses imply the boundedness of the derivatives of each order due to Cauchy’s estimate in several variables (see e.g., Section 1.3 of [48]). It is noted that the k -th derivatives of the vector fields in Example 1 and Example 2 are $\mathcal{O}(1/h^k)$. Thus the hypotheses on the target governing function f and the learned network f_θ exclude the targets and the solutions containing high-frequency components similar to those in Example 1 and Example 2, respectively. The analyticity hypothesis on the target governing function implies our analysis is restricted to the discovery of low-frequency dynamics. In addition, as discussed in [15], it is natural to conjecture that the implicit regularization that neural networks fit targets from low to high frequencies during gradient descent can be applied to LMNets. If the target system is analytic, the gradient descent is expected to converge to an analytic solution without high-frequency components. Therefore, the analyticity hypothesis on the learned network is reasonable.

4.2 Proofs

We present the proof of Theorem 2 in this subsection. The proof will be divided into three parts: First, we estimate the upper bounds of the Lie derivatives $\mathbf{D}^k g$ and the expansion terms f_k of the IMDE, which are used as a cornerstone for the subsequent estimations. In addition, we prove that

$$\sum_{m=0}^M \alpha_m \phi_{mh,f}(x) - h \sum_{m=0}^M \beta_m f_h^K(\phi_{mh,f}(x))$$

can be made exponentially small by choosing appropriate truncation index K . Finally we present the upper bound of the difference between the learned model f_θ and the truncated IMDE f_h^K , and thereby conclude the proof. The proofs are based on the recursion formula (16) and Cauchy’s estimate [9].

We start with the following auxiliary lemma.

Lemma 1. *Suppose g that are analytic and bounded in $\mathcal{B}(\Omega, r)$, then*

$$\|g'(y)\| \leq \|g\|_{\mathcal{B}(\Omega, r)} / r$$

for any $y \in \Omega$ in the operator norm.

Proof. For $y \in \Omega$ and $\|\Delta y\| \leq 1$, the function $\alpha(z) = g(y + z\Delta y)$ is analytic for $|z| \leq r$ and bounded by $\|g\|_{\mathcal{B}(\Omega, r)}$. By Cauchy’s estimate, we obtain

$$\|g'(y)\Delta y\| = \|\alpha'(0)\| \leq \|g\|_{\mathcal{B}(\Omega, r)} / r,$$

and thus conclude the proof. □

By this auxiliary lemma, we immediately conclude the bound of Lie derivatives, which will be used frequently.

Lemma 2. *Suppose f, g that are analytic and bounded in $\mathcal{B}(\Omega, r)$, then*

$$(1) \quad \|\mathbf{D}^k g\|_{\Omega} \leq \|g\|_{\mathcal{B}(\Omega, r)} \left(\frac{k \|f\|_{\mathcal{B}(\Omega, r)}}{r} \right)^k ;$$

$$(2) \quad \|\mathbf{D}^k g\|_{\Omega} \leq k! \|g\|_{\mathcal{B}(\Omega, r)} \left(\frac{e \|f\|_{\mathcal{B}(\Omega, r)}}{r} \right)^k .$$

Proof. For fixed index \hat{k} , we will obtain the desired estimate $\|\mathbf{D}^{\hat{k}} g\|_{\Omega}$ via estimating

$$\|\mathbf{D}^k g\|_{\mathcal{B}(\Omega, (1-k/\hat{k})r)}, \text{ for } k = 0, 1, \dots, \hat{k}.$$

In the following we abbreviate $\|\cdot\|_{\mathcal{B}(\Omega, (1-k/\hat{k})r)}$ by $\|\cdot\|_k$.

According to Lemma 1, we have

$$\|\mathbf{D}^k g\|_k = \|\mathbf{D}(\mathbf{D}^{k-1} g)\|_k = \|(\mathbf{D}^{k-1} g)' f\|_k \leq \frac{\hat{k}}{r} \|\mathbf{D}^{k-1} g\|_{k-1} \|f\|_k .$$

Using this estimate iteratively, together with the fact that $\|f\|_k \leq \|f\|_{\mathcal{B}(\Omega, r)}$, we conclude that

$$\|\mathbf{D}^{\hat{k}} g\|_{\hat{k}} \leq \|g\|_0 \left(\frac{\hat{k} \|f\|_{\mathcal{B}(\Omega, r)}}{r} \right)^{\hat{k}},$$

which completes the first part of the proof.

Finally, according to Stirling's formula that $k^k \leq k!e^k$, we immediately complete the second part of the proof. \square

Next, we rewrite the recursion formula (16) and give an upper bound of f_k .

Lemma 3. *The expansion terms f_k defined by (16) satisfy*

$$f_k(y) = \xi_k(\mathbf{D}^k f)(y),$$

where

$$\xi_0 = 1, \quad \xi_k = \sum_{m=0}^M \alpha_m \frac{m^{k+1}}{(k+1)!} - \sum_{m=0}^M \beta_m \sum_{j=1}^k \frac{m^j}{j!} \xi_{k-j}, \text{ for } k \geq 1. \quad (19)$$

Furthermore, if f is analytic and bounded in $\mathcal{B}(\Omega, r)$, then, the expansion terms f_k satisfy

$$\|f_k\|_{\mathcal{B}(\Omega, r/2)} \leq \mu \|f\|_{\mathcal{B}(\Omega, r)} \left(\frac{\eta k \|f\|_{\mathcal{B}(\Omega, r)}}{r} \right)^k,$$

where constants μ and η depend only on the coefficients α_m and β_m of the LMM.

Proof. We first prove the first part by induction on $k \geq 0$. First, the case when $k = 0$ is obvious. Suppose now that the statement holds for $k \leq K - 1$. Then, by the recursion formula (16) and the inductive hypothesis, we have

$$\begin{aligned} f_K(y) &= \sum_{m=0}^M \alpha_m \frac{m^{K+1}}{(K+1)!} (\mathbf{D}^K f)(y) - \sum_{m=0}^M \beta_m \sum_{j=1}^K \frac{m^j}{j!} (\mathbf{D}^j f_{K-j})(y) \\ &= \sum_{m=0}^M \alpha_m \frac{m^{K+1}}{(K+1)!} (\mathbf{D}^K f)(y) - \sum_{m=0}^M \beta_m \sum_{j=1}^K \frac{m^j}{j!} \xi_{K-j} (\mathbf{D}^K f)(y) \\ &= \xi_K (\mathbf{D}^K f)(y), \end{aligned}$$

which completes the induction and thus concludes the first part of the proof.

Let $\Xi(z) = \sum_{k=1}^{\infty} \xi_k z^k$, $z \in \mathbb{C}$. By multiplying (19) with z^k and summing over $k \geq 1$, we obtain that

$$\Xi(z) = \sum_{k=1}^{\infty} z^k \sum_{m=0}^M \alpha_m \frac{m^{k+1}}{(k+1)!} - \sum_{k=1}^{\infty} z^k \sum_{m=0}^M \beta_m \sum_{j=1}^k \frac{m^j}{j!} \xi_{k-j}.$$

By interchanging the summation order, we have

$$\begin{aligned} \Xi(z) &= \sum_{m=0}^M \alpha_m \sum_{k=1}^{\infty} \frac{m^{k+1}}{(k+1)!} z^k - \sum_{m=0}^M \beta_m \sum_{k=1}^{\infty} z^k \sum_{j=1}^k \frac{m^j}{j!} \xi_{k-j} \\ &= \sum_{m=0}^M \alpha_m \sum_{k=1}^{\infty} \frac{m^{k+1}}{(k+1)!} z^k - \sum_{m=0}^M \beta_m \sum_{j=1}^{\infty} \frac{m^j}{j!} z^j \sum_{k=j}^{\infty} \xi_{k-j} z^{k-j} \\ &= \sum_{m=0}^M \alpha_m (e^{mz} - 1 - mz)/z + \sum_{m=0}^M \beta_m (1 - e^{mz})(\Xi(z) + 1). \end{aligned}$$

Using the fact that $\sum_{m=0}^M \beta_m = \sum_{m=0}^M m \cdot \alpha_m = 1$, we conclude that

$$\Xi(z) + 1 = \frac{\sum_{m=0}^M \alpha_m (e^{mz} - 1)/z}{\sum_{m=0}^M \beta_m e^{mz}}.$$

In addition, since $(\sum_{m=0}^M \beta_m e^{mz})|_{z=0} = 1$, there exists a constant $\hat{Z} < 1$ such that $|\sum_{m=0}^M \beta_m e^{mz}| \geq 1/2$ for $|z| \leq \hat{Z}$. Therefore, we have that

$$|\Xi(z) + 1| \leq 2\hat{\mu}, \text{ for } |z| \leq \hat{Z}, \text{ where } \hat{\mu} = \max_{|z| \leq \hat{Z}} \left| \sum_{m=0}^M \alpha_m (e^{mz} - 1)/z \right|.$$

By Cauchy's estimate, together with the fact that $k! \xi_k = \Xi^{(k)}(0)$, we deduce that $\xi_k \leq 2\hat{\mu}/\hat{Z}^k$. Finally, by the first term of Lemma 2, and taking $\mu = 2\hat{\mu}$, $\eta = 2/\hat{Z} > 1$, we conclude that

$$\|f_k\|_{\mathcal{B}(\Omega, r/2)} \leq \mu \|f\|_{\mathcal{B}(\Omega, r)} \left(\frac{\eta k \|f\|_{\mathcal{B}(\Omega, r)}}{r} \right)^k.$$

The proof is completed. \square

The following lemma is analogous to Theorem 2 in [20]. The latter shows the rigorous exponentially small error estimates for the modified differential equation of LMMs. Our proof, as well as the proofs of Lemma 2 and 3, is also inspired by theirs and other analyses for modified differential equations [2, 21, 44].

Lemma 4. *Suppose f is analytic and bounded in $\mathcal{B}(\Omega, r)$. Let $\gamma_0 = \frac{r}{(e\eta\|f\|_{\mathcal{B}(\Omega, r)})}$, and let K be the largest integer satisfying $hK \leq \gamma_0$. If $h \leq \eta\gamma_0/(2eM)$, the truncated IMDE satisfies*

$$\left\| \sum_{m=0}^M \alpha_m \phi_{mh, f}(\cdot) - h \sum_{m=0}^M \beta_m f_h^K(\phi_{mh, f}(\cdot)) \right\|_{\Omega} \leq \rho h \|f\|_{\mathcal{B}(\Omega, r)} e^{-\gamma_0/h},$$

where ρ depends only on the coefficients α_m and β_m of the LMM.

Proof. First, by using (13) with substituting $t = mh$ and $F(y) = f_h(y)$, we have that

$$\begin{aligned} & h \sum_{m=0}^M \beta_m f_h^K(\phi_{mh, f}(x)) \\ &= h \sum_{m=0}^M \beta_m \sum_{i=0}^K \sum_{j=0}^{\infty} \frac{(mh)^j}{j!} h^i (\mathbf{D}^j f_i)(x) \\ &= h \sum_{m=0}^M \beta_m \sum_{i=0}^K \sum_{j=0}^{K-i} \frac{(mh)^j}{j!} h^i (\mathbf{D}^j f_i)(x) + h \sum_{m=0}^M \beta_m \sum_{i=0}^K \sum_{j=K-i+1}^{\infty} \frac{(mh)^j}{j!} h^i (\mathbf{D}^j f_i)(x) \\ &=: \mathcal{F}_{\leq K+1}^{\beta}(x) + \mathcal{F}_{> K+1}^{\beta}(x). \end{aligned}$$

According to the second term of Lemma 2 and Lemma 3, we deduce that

$$\begin{aligned} \|\mathbf{D}^j f_i\|_{\Omega} &\leq j! \|f_i\|_{\mathcal{B}(\Omega, r/2)} \left(\frac{2e \|f\|_{\mathcal{B}(\Omega, r/2)}}{r} \right)^j \\ &\leq j! \mu \|f\|_{\mathcal{B}(\Omega, r)} \left(\frac{\eta i \|f\|_{\mathcal{B}(\Omega, r)}}{r} \right)^i \left(\frac{2e \|f\|_{\mathcal{B}(\Omega, r)}}{r} \right)^j. \end{aligned}$$

This estimate implies that

$$\left\| \mathcal{F}_{> K+1}^{\beta} \right\|_{\Omega} \leq \mu h \|f\|_{\mathcal{B}(\Omega, r)} \sum_{m=0}^M |\beta_m| \sum_{i=0}^K \left(\frac{\eta i h \|f\|_{\mathcal{B}(\Omega, r)}}{r} \right)^i \sum_{j=K-i+1}^{\infty} \left(\frac{2emh \|f\|_{\mathcal{B}(\Omega, r)}}{r} \right)^j.$$

Since $2emh \|f\|_{\mathcal{B}(\Omega, r)} / r \leq 1/e$, we have that

$$\left\| \mathcal{F}_{> K+1}^{\beta} \right\|_{\Omega} \leq \frac{e\mu}{e-1} h \|f\|_{\mathcal{B}(\Omega, r)} \sum_{m=0}^M |\beta_m| \sum_{i=0}^K \left(\frac{\eta i h \|f\|_{\mathcal{B}(\Omega, r)}}{r} \right)^i e^{i-K-1}.$$

Therefore, according to the property of K that $hK \leq \gamma_0$, we obtain that

$$\left\| \mathcal{F}_{> K+1}^{\beta} \right\|_{\Omega} \leq \frac{e\mu}{e-1} h \|f\|_{\mathcal{B}(\Omega, r)} \sum_{m=0}^M |\beta_m| \sum_{i=0}^K \left(\frac{i}{K} \right)^i e^{-K-1}.$$

By observing the facts

$$\frac{1}{K} + \left(\frac{2}{K}\right)^2 > \frac{1}{K+1} + \left(\frac{2}{K+1}\right)^2 + \left(\frac{3}{K+1}\right)^3, \quad \text{for } K \geq 7,$$

and

$$\left(\frac{i}{K}\right)^i \geq \left(\frac{i+1}{K+1}\right)^{i+1}, \quad \text{for } 1 \leq i \leq K,$$

we deduce that the sum $\sum_{i=0}^K (i/K)^i$ is maximal for $K = 6$ and bounded by 2.01. Combining these estimations, together with the property of K that $h(K+1) > \gamma_0$, we thus conclude that

$$\left\| \mathcal{F}_{>K+1}^\beta \right\|_\Omega \leq \rho_\beta h \|f\|_{\mathcal{B}(\Omega, r)} e^{-\gamma_0/h}, \quad \text{where } \rho_\beta = \frac{2.01e\mu}{e-1} \sum_{m=0}^M |\beta_m|. \quad (20)$$

In addition, using formula (14), we have

$$\begin{aligned} \sum_{m=0}^M \alpha_m \phi_{mh, f}(x) &= \sum_{m=0}^M \alpha_m \sum_{k=0}^{K+1} \frac{(mh)^k}{k!} (\mathbf{D}^k I_D)(x) + \sum_{m=0}^M \alpha_m \sum_{k=K+2}^{\infty} \frac{(mh)^k}{k!} (\mathbf{D}^k I_D)(x) \\ &=: \mathcal{F}_{\leq K+1}^\alpha + \mathcal{F}_{>K+1}^\alpha. \end{aligned}$$

By the second term of Lemma 2 and the fact that $\mathbf{D}^k I_D = \mathbf{D}^{k-1} f$, we deduce that

$$\begin{aligned} \left\| \mathcal{F}_{>K+1}^\alpha \right\|_\Omega &\leq h \|f\|_{\mathcal{B}(\Omega, r)} \sum_{m=0}^M |\alpha_m| m \sum_{k=K+2}^{\infty} \left(\frac{emh \|f\|_{\mathcal{B}(\Omega, r)}}{r} \right)^{k-1} \\ &\leq \rho_\alpha h \|f\|_{\mathcal{B}(\Omega, r)} e^{-\gamma_0/h}, \end{aligned} \quad (21)$$

with $\rho_\alpha = \frac{2e}{2e-1} \sum_{m=0}^M 2^{-2eM/\eta} |\alpha_m| m$. Here, we again use the fact that

$$2emh \|f\|_{\mathcal{B}(\Omega, r)} / r \leq 1/e, \quad K+1 \geq 2eM/\eta, \quad \text{and } e^{-(K+1)} \leq e^{-\gamma_0/h}.$$

Finally, due to the definition of IMDE, we have that

$$\sum_{m=0}^M \alpha_m \phi_{mh, f}(x) - h \sum_{m=0}^M \beta_m f_h^K(\phi_{mh, f}(x)) = \mathcal{F}_{>K+1}^\alpha + \mathcal{F}_{>K+1}^\beta.$$

Therefore, by combining estimates (20) and (21) we conclude that

$$\begin{aligned} \left\| \sum_{m=0}^M \alpha_m \phi_{mh, f}(\cdot) - h \sum_{m=0}^M \beta_m f_h^K(\phi_{mh, f}(\cdot)) \right\|_\Omega &\leq \left\| \mathcal{F}_{>K+1}^\alpha \right\|_\Omega + \left\| \mathcal{F}_{>K+1}^\beta \right\|_\Omega \\ &\leq \rho h \|f\|_{\mathcal{B}(\Omega, r)} e^{-\gamma_0/h}, \end{aligned}$$

where $\rho = \rho_\alpha + \rho_\beta$ depends only on the coefficients α_m and β_m . \square

Again using Lemma 3, we can give the following lemma, which yields upper bounds of f_h^K and $f_h^K - f$ immediately.

Lemma 5. *Suppose f is analytic and bounded in $\mathcal{B}(\Omega, r)$. Let $\gamma_0 = \frac{r}{(e\eta\|f\|_{\mathcal{B}(\Omega, r)})}$, and let K be the largest integer satisfying $hK \leq \gamma_0$. Then for integer p with $0 \leq p \leq K$, the truncated IMDE satisfies*

$$\left\| \sum_{k=p}^K h^k f_k \right\|_{\mathcal{B}(\Omega, r/2)} \leq \mu \|f\|_{\mathcal{B}(\Omega, r)} \left(\frac{\eta \|f\|_{\mathcal{B}(\Omega, r)}}{r} \right)^p d_p h^p,$$

where d_p depends only on p .

Proof. From Lemma 3, we obtain that

$$\left\| \sum_{k=p}^K h^k f_k \right\|_{\mathcal{B}(\Omega, r/2)} \leq \sum_{k=p}^K h^k \mu \|f\|_{\mathcal{B}(\Omega, r)} \left(\frac{\eta k \|f\|_{\mathcal{B}(\Omega, r)}}{r} \right)^k.$$

Since $h \leq r/(Ke\eta\|f\|_{\mathcal{B}(\Omega, r)})$, we deduce that

$$\left\| \sum_{k=p}^K h^k f_k \right\|_{\mathcal{B}(\Omega, r/2)} \leq h^p \mu \|f\|_{\mathcal{B}(\Omega, r)} \left(\frac{\eta \|f\|_{\mathcal{B}(\Omega, r)}}{r} \right)^p \sum_{k=p}^K \left(\frac{k}{eK} \right)^k K^p.$$

Observing that $\left(\frac{k}{eK}\right)^k$ is decreasing for k on the interval $[p+1, K]$, we have that

$$\begin{aligned} \sum_{k=p}^K \left(\frac{k}{eK} \right)^k &\leq \left(\frac{p}{eK} \right)^p + (K-p) \left(\frac{p+1}{eK} \right)^{p+1} \\ &\leq \left[\left(\frac{p}{e} \right)^p + \left(\frac{p+1}{e} \right)^{p+1} \right] K^{-p} =: d_p K^{-p}. \end{aligned}$$

Therefore we conclude that

$$\left\| \sum_{k=p}^K h^k f_k \right\|_{\mathcal{B}(\Omega, r/2)} \leq \mu \|f\|_{\mathcal{B}(\Omega, r)} \left(\frac{\eta \|f\|_{\mathcal{B}(\Omega, r)}}{r} \right)^p d_p h^p.$$

The proof is completed. □

Corollary 2. *Under notations and conditions of Lemma 5, the truncated IMDE satisfies*

$$\|f_h^K\|_{\mathcal{B}(\Omega, r/2)} \leq (1 + e^{-1})\mu \|f\|_{\mathcal{B}(\Omega, r)}.$$

Corollary 3. *Under notations and conditions of Lemma 5, if the LMM is of order p , then, the truncated IMDE satisfies*

$$\|f_h^K - f\|_{\mathcal{B}(\Omega, r/2)} \leq \mu \|f\|_{\mathcal{B}(\Omega, r)} \left(\frac{\eta \|f\|_{\mathcal{B}(\Omega, r)}}{r} \right)^p d_p h^p,$$

where d_p depends only on p .

With these results, we are able to provide the proof of the main theorem.

Proof of Theorem 2. From Lemma 4 with taking $\Omega = \mathcal{B}(x, r_1)$ and $r = r_2$, we know that for sufficiently small h ,

$$\left\| \sum_{m=0}^M \alpha_m \phi_{mh, f}(\cdot) - h \sum_{m=0}^M \beta_m f_h^K(\phi_{mh, f}(\cdot)) \right\|_{\mathcal{B}(x, r_1)} \leq \rho h b_2 e^{-\gamma_0/h}.$$

And thus we have

$$\delta := \left\| \sum_{m=0}^M \beta_m f_h^K(\phi_{mh, f}(\cdot)) - \sum_{m=0}^M \beta_m f_\theta(\phi_{mh, f}(\cdot)) \right\|_{\mathcal{B}(x, r_1)} \leq \mathcal{L} + \rho b_2 e^{-\gamma_0/h}. \quad (22)$$

According to Equation (13), we obtain that

$$\sum_{m=0}^M \beta_m f_h^K(\phi_{mh, f}(x)) - \sum_{m=0}^M \beta_m f_\theta(\phi_{mh, f}(x)) = \sum_{m=0}^M \beta_m \sum_{j=0}^{\infty} \frac{(mh)^j}{j!} \mathbf{D}^j(f_h^K - f_\theta)(x).$$

Let $h_1 = (\sum_{m=0}^M |\beta_m| e + 1)h$, for integer i with $1 \leq i + 1 \leq r_1/(eMh_1b_1)$, according to the second term of Lemma 2, we have that

$$\left\| \mathbf{D}^j(f_h^K - f_\theta) \right\|_{\mathcal{B}(x, eiMh_1b_1)} \leq j! \left\| f_h^K - f_\theta \right\|_{\mathcal{B}(x, e(i+1)Mh_1b_1)} (Mh_1)^{-j}.$$

Thus we obtain that

$$\begin{aligned} \delta &\geq \left\| (f_h^K - f_\theta)(\cdot) + \sum_{m=0}^M \beta_m \sum_{j=1}^{\infty} \frac{(mh)^j}{j!} \mathbf{D}^j(f_h^K - f_\theta)(\cdot) \right\|_{\mathcal{B}(x, eiMh_1b_1)} \\ &\geq \left\| f_h^K - f_\theta \right\|_{\mathcal{B}(x, eiMh_1b_1)} - \left\| f_h^K - f_\theta \right\|_{\mathcal{B}(x, e(i+1)Mh_1b_1)} \sum_{m=0}^M |\beta_m| \sum_{j=1}^{\infty} \left(\frac{h}{h_1} \right)^j \\ &\geq \left\| f_h^K - f_\theta \right\|_{\mathcal{B}(x, eiMh_1b_1)} - e^{-1} \left\| f_h^K - f_\theta \right\|_{\mathcal{B}(x, e(i+1)Mh_1b_1)}, \end{aligned}$$

which yields that

$$\left\| f_h^K - f_\theta \right\|_{\mathcal{B}(x, eiMh_1b_1)} - \frac{\delta}{1 - e^{-1}} \leq e^{-1} \left(\left\| f_h^K - f_\theta \right\|_{\mathcal{B}(x, e(i+1)Mh_1b_1)} - \frac{\delta}{1 - e^{-1}} \right).$$

By using this estimation iteratively, together with Corollary 2, we deduce that

$$\begin{aligned} \left\| f_h^K(x) - f_\theta(x) \right\| &\leq \frac{\delta}{1 - e^{-1}} + e^{-\gamma_1/h+1} \left(\left\| f_h^K - f_\theta \right\|_{\mathcal{B}(x, r_1)} - \frac{\delta}{1 - e^{-1}} \right) \\ &\leq \frac{\delta}{1 - e^{-1}} + c' e^{-\gamma_1/h}, \end{aligned}$$

where $\gamma_1 = \frac{r_1}{2Mb_1(\sum_{m=0}^M |\beta_m| e + 1)}$, $c' = (e + 1)\mu b_2 + b_1$. Combining it and the definition of δ (22), we conclude that

$$\left\| f_h^K(x) - f_\theta(x) \right\| \leq \frac{\mathcal{L}}{1 - e^{-1}} + c_1 b_2 \cdot e^{-\gamma/h},$$

where constant γ and c_1 depend only on r_1/b_1 , r_2/b_2 and the coefficients α_m and β_m .

Finally, we immediately derive the bound of $\|f_\theta - f\|$ by using Corollary 3 and the triangle inequality. The proof is completed. \square

5 Numerical experiments

In this section, we present various numerical evidence of the discovery of hidden dynamics using LMNets to demonstrate that the order of accuracy is consistent with the theoretical findings. Following [15, 32, 43], we consider three benchmark problems, including the damped oscillator problem, the Lorenz system and the glycolytic oscillator, but use different settings from prior results [15, 32, 43] to avoid duplication and highlight our analysis. Here we test the error orders of AB, BDF, and AM schemes for discovery, whose coefficients can be found in [24].

As shown in Theorem 2, the total error is affected by the discretization error and the learning loss. To measure the learning performance, we sample the test data \mathcal{T}_{test} in the same form and manner as the training data, i.e.,

$$\mathcal{T}_{test} = \left\{ \left(x_n^{test}, \phi_{h,f}(x_n^{test}), \dots, \phi_{Mh,f}(x_n^{test}) \right) \right\}_{n=1}^{N_{test}},$$

and calculate the average test loss in the l_∞ - norm, which is formulated as

$$\text{Test loss} = \frac{1}{N_{test}} \sum_{n=1}^{N_{test}} \left\| \sum_{m=0}^M h^{-1} \alpha_m \phi_{mh,f}(x_n^{test}) - \sum_{m=0}^M \beta_m f_\theta(\phi_{mh,f}(x_n^{test})) \right\|.$$

In practice, we can split our data into two: a training dataset for optimizing loss and a test dataset for measuring learning performance. In addition, we evaluate the average error in the l_∞ - norm, i.e.,

$$\text{Error}(g_1, g_2) = \frac{1}{|\mathcal{T}|} \sum_{x_i \in \mathcal{T}} \|g_1(x_i) - g_2(x_i)\|, \quad (23)$$

where \mathcal{T} is composed of several points randomly sampled from the given compact region in the first example, and is composed of all the initial states in the test data in the second and third examples, i.e., $\mathcal{T} = \{x_n^{test}\}_{n=1}^{N_{test}}$. In all examples, we use the fourth-order RK method on a very fine mesh to generate data and simulate the discovered systems for numerical validation. All neural network models are trained on the PyTorch framework with Tesla P40 GPU, where Python 3.8 environment and CUDA 10.1 toolkit are utilized.

5.1 Damped oscillator problem

To begin with, we consider the damped harmonic oscillator with cubic dynamics. The system of equation for $y = (p, q)$ is given by

$$\frac{d}{dt}p = -0.1p^3 + 2.0q^3, \quad \frac{d}{dt}q = -2.0p^3 - 0.1q^3. \quad (24)$$

We generate 1500 and 500 trajectories for the training and test data, respectively. For each trajectory, the initial state is randomly sampled from $[-2.2, 2.2] \times [-2.2, 2.2]$ and 10 subsequent states at equidistant time steps h are collected. The neural networks employed consist of two hidden layers with 128 units and `tanh` activation. We optimize the training loss using full batch for 10^5 epochs, where the optimizer is chosen to be Adam optimization [33] in the Pytorch library, and the learning rate is set to decay exponentially with linearly decreasing powers from 10^{-2} to 10^{-4} .

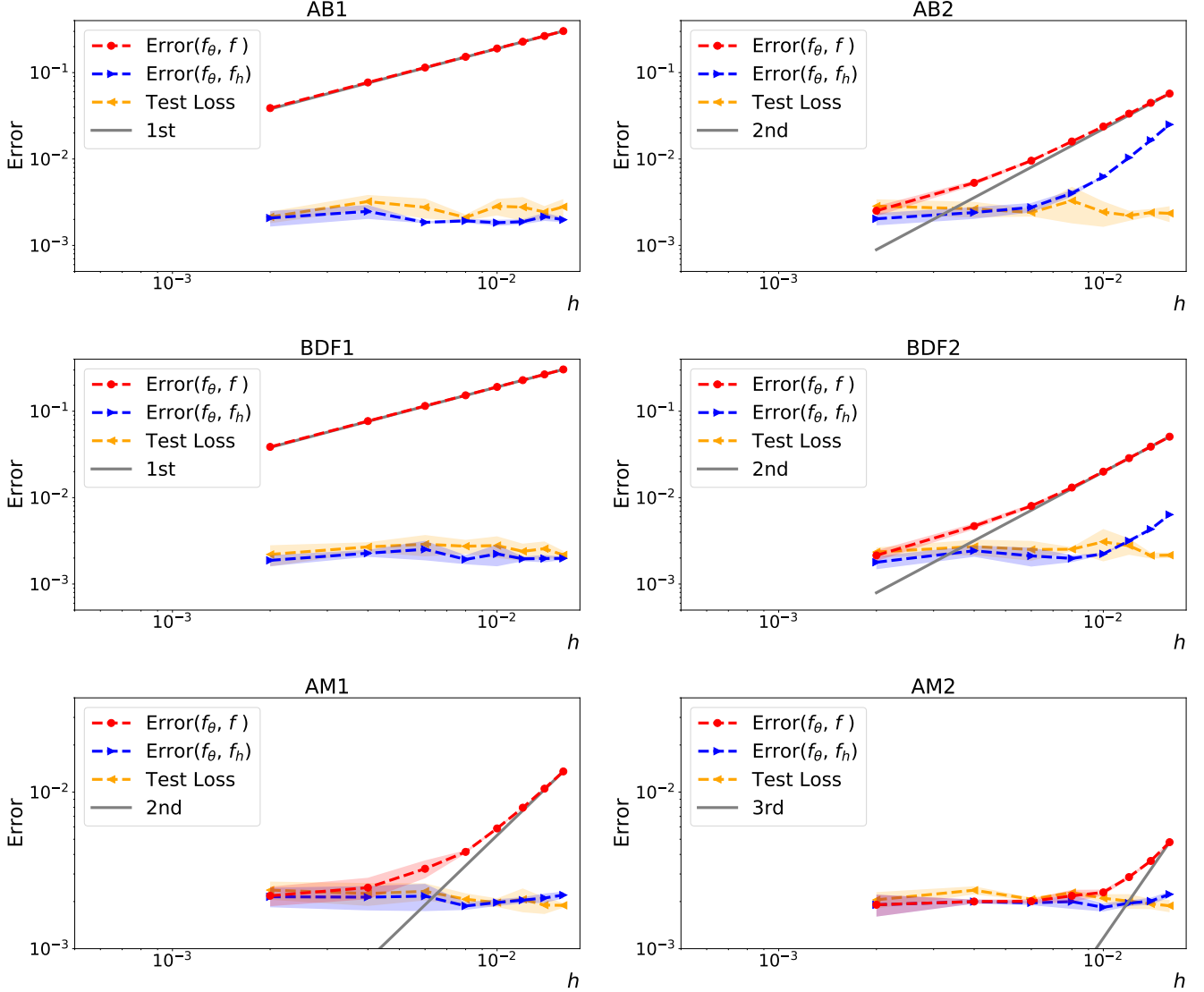


Figure 1: $\text{Error}(f_\theta, f)$, $\text{Error}(f_\theta, f_h)$ and test loss versus h for the damped harmonic oscillator (24). The results are obtained by taking the mean of 5 independent experiments, and the shaded region represents one standard deviation.

We first verify the convergence rate with respect to step size h of LMNets. Since the total error depends on the learning loss on the neighborhood, we randomly sample 10^4 points from $[-2, 2] \times [-2, 2]$ as \mathcal{T} , and evaluate the error between f_θ and f , and the error between f_θ and f_h^4 according to (23). The error versus steps h (assigned as $h = 0.002n, n = 1, \dots, 8$) and schemes (AB, BDF, AM) is presented in Fig. 1. Here, 5 independent experiments are performed for each case to obtain the means and the standard deviations. It is shown in Fig. 1 that the error order is consistent with the order of the employed LMM when the discretization error is dominated (see AB1, BDF1 and AB2, BDF2, AM1 with large h). And learning loss dominates the total error when using accurate LMM schemes (see AB2, BDF2, AM1 with small h and AM2). These numerical results indicate that the total error is affected by the discretization error Ch^p and the learning loss

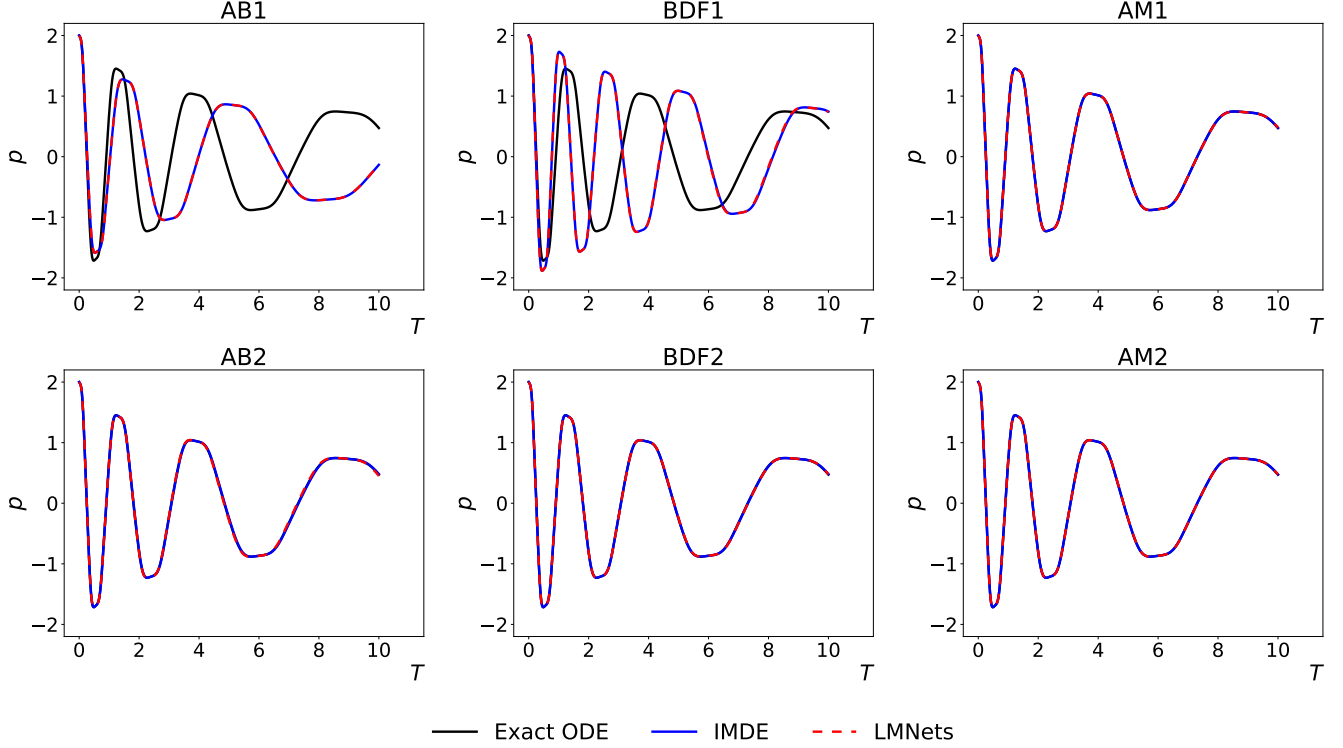


Figure 2: The first component of the trajectories of exact, modified and discovered systems for the damped harmonic oscillator (24).

when using an LMM of order p , which support the theoretical analysis of this paper.

In addition, Fig. 1 also shows that the error between f_h and f_θ is significantly lower than that between f and f_θ . Despite that we only use truncation f_h^4 here, the error between f_h and f_θ is almost close to learning loss except for AB2. Moreover, we simulate the discovered system $\frac{d}{dt}y = f_\theta(y)$, the exact system (24) and the truncated IMDE $\frac{d}{dt}y = f_h^4(y)$ starting at $(2, 0)$. The first components of these trajectories are plotted in Fig. 2 for comparison. It can be observed that the discovered dynamical systems accurately capture the evolution of the corresponding IMDE when using LMMs of order 1. And LMNets successfully learn the target system when the IMDE is close to the target system (AB2, BDF2, AM1 and AM2). These results indicate that training LMNets returns an approximation of the IMDE, which are consistent with the theoretical conclusions in Theorem 2.

5.2 Lorenz system

Subsequently, we consider the normalized 3-D Lorenz system [37, 50], which is a simplified model for atmospheric dynamics and is given as

$$\frac{d}{dt}p = 10(q - p), \quad \frac{d}{dt}q = p(28 - 10r) - q, \quad \frac{d}{dt}r = 10pq - \frac{8}{3}r, \quad (25)$$

where $y = (p, q, r)$. Here, the training data consists of data points on a single trajectory from $t = 0$ to $t = 10$ with data step h and initial condition $y_0 = (-0.8, 0.7, 2.7)$,

$$\mathcal{T}_{train} = \{(x_n, \phi_{h,f}(x_n), \dots, \phi_{Mh,f}(x_n)) | x_n = \phi_{nh}(y_0), n = 0, 1, \dots, 10/h - M\},$$

and the test data is set as

$$\mathcal{T}_{test} = \{(x_n, \phi_{h,f}(x_n), \dots, \phi_{Mh,f}(x_n)) | x_n = \phi_{n\hat{h}}(y_0), n = 0, 1, \dots, (10 - Mh)/\hat{h}\},$$

where $\hat{h} = 0.002$. The chosen model architecture and hyper-parameters are the same as in subsection 5.1 except that the total number of epochs is set as 3×10^5 .

Table 1: Quantitative results of the Lorenz system (25) obtained by AB and BDF schemes.

Schemes		AB			BDF		
M	h	Test Loss	Error	Order	Test Loss	Error	Order
1	0.002	2.218e-03	9.521e-02	—	2.236e-03	9.522e-02	—
	0.004	2.352e-03	1.904e-01	1.000	2.228e-03	1.904e-01	1.000
	0.008	2.385e-03	3.806e-01	0.999	2.302e-03	3.808e-01	1.000
	0.016	8.453e-03	7.606e-01	0.999	7.107e-03	7.614e-01	1.000
	0.032	7.947e-02	1.507e+00	0.986	5.945e-02	1.523e+00	1.000
2	0.002	2.267e-03	3.891e-03	—	2.385e-03	3.547e-03	—
	0.004	2.306e-03	1.182e-02	1.602	2.271e-03	9.753e-03	1.459
	0.008	2.386e-03	4.561e-02	1.949	2.361e-03	3.714e-02	1.929
	0.016	9.148e-03	1.770e-01	1.957	7.383e-03	1.478e-01	1.993
	0.032	7.804e-02	6.420e-01	1.858	7.836e-02	5.703e-01	1.948
3	0.002	2.275e-03	2.315e-03	—	2.278e-03	2.374e-03	—
	0.004	2.353e-03	2.935e-03	0.342	2.252e-03	2.857e-03	0.267
	0.008	2.447e-03	1.101e-02	1.907	2.266e-03	8.208e-03	1.522
	0.016	1.242e-02	7.151e-02	2.699	8.175e-03	5.146e-02	2.648
	0.032	8.844e-02	4.480e-01	2.647	8.036e-02	3.269e-01	2.667

Table 2: Quantitative results of the Lorenz system (25) obtained by AM schemes.

Schemes	AM1			AM2		
h	Test Loss	Error	Order	Test Loss	Error	Order
0.002	2.323e-03	2.453e-03	—	2.368e-03	2.393e-03	—
0.004	2.305e-03	3.518e-03	0.520	2.288e-03	2.397e-03	0.002
0.008	2.366e-03	9.828e-03	1.482	2.445e-03	3.304e-03	0.463
0.016	6.845e-03	3.972e-02	2.015	5.778e-03	1.416e-02	2.099
0.032	6.707e-02	1.747e-01	2.137	6.852e-02	1.096e-01	2.952

We first test the convergence with respect to data step size h for AB and BDF schemes. We calculate the error on the test data and record the error as well as the test loss in Table 1 to show the convergence more clearly. Here, 5 independent experiments are simulated to obtain the means.

Table 3: Leading terms of $f_h - f$.

Schemes	AB2	BDF2	AM1	AB3	BDF2	AM2
Leading terms	$\frac{5h^2}{12}\mathbf{D}^2 f$	$-\frac{h^2}{3}\mathbf{D}^2 f$	$-\frac{h^2}{12}\mathbf{D}^2 f$	$\frac{3h^3}{8}\mathbf{D}^3 f$	$-\frac{h^3}{4}\mathbf{D}^3 f$	$-\frac{h^3}{24}\mathbf{D}^3 f$

As discussed and numerically verified in [15], LMNets without the auxiliary conditions perform well when h is small. Thus we only take relatively small h . It is shown in Table 1 that there exists a threshold caused by the learning loss, and LMNets can effectively discover the hidden dynamics with an error order consistent with the theoretical ones when the error is significantly larger than the test loss.

Moreover, we test the performance of AM schemes using the same settings and report the quantitative results in Table 2. Despite that LMNets with AM are unstable for discovery [15], they can still perform well and the same error phenomenon can be observed, which is also consistent with the theoretical analysis. It is observed that the error of LMNets using AM is smaller than that using AB and BDF schemes of the same order, which is due to the different leading terms of $f_h - f$ (obtained by Corollary 1 and presented in Table 3).

5.3 Glycolytic oscillator

Finally, we consider the model of oscillations in yeast glycolytic. The model describes the concentrations of 7 biochemical species and is formulated as

$$\begin{aligned}
\frac{d}{dt}S_1 &= J_0 - \frac{k_1 S_1 S_6}{1 + (S_6/K_1)^q}, \\
\frac{d}{dt}S_2 &= 2\frac{k_1 S_1 S_6}{1 + (S_6/K_1)^q} - k_2 S_2 (N - S_5) - k_6 S_2 - 2S_5, \\
\frac{d}{dt}S_3 &= k_2 S_2 (N - S_5) - k_3 S_3 (A - S_6), \\
\frac{d}{dt}S_4 &= k_3 S_3 (A - S_6) - k_4 S_4 S_5 - \kappa(S_4 - S_7), \\
\frac{d}{dt}S_5 &= k_2 S_2 (N - S_5) - k_4 S_4 S_5 - k_6 S_2 S_5, \\
\frac{d}{dt}S_6 &= -2\frac{k_1 S_1 S_6}{1 + (S_6/K_1)^q} + 2k_3 S_3 (A - S_6) - k_5 S_6, \\
\frac{d}{dt}S_7 &= \psi \kappa(S_4 - S_7) - k S_7,
\end{aligned} \tag{26}$$

where $y = (S_1, \dots, S_7)$ and the parameters are taken from Table 1 in [13]. We simulate 60 and 40 trajectories ($T = 10$) for the training and test data, respectively. For each trajectory, the initial state is randomly sampled from half of the ranges provided in table 2 of [13]. The chosen model architecture and hyper-parameters are the same as in subsection 5.2 except the batch size is set as 3×10^4 .

We continue to test the convergence of LMNets using AB, BDF and AM schemes with respect to h (assigned as $h = 0.002 * 2^n, n = 0, \dots, 4$), where the error is evaluated on the test data. The error and the test loss versus h is shown in Fig. 1. It is shown that the convergence rates

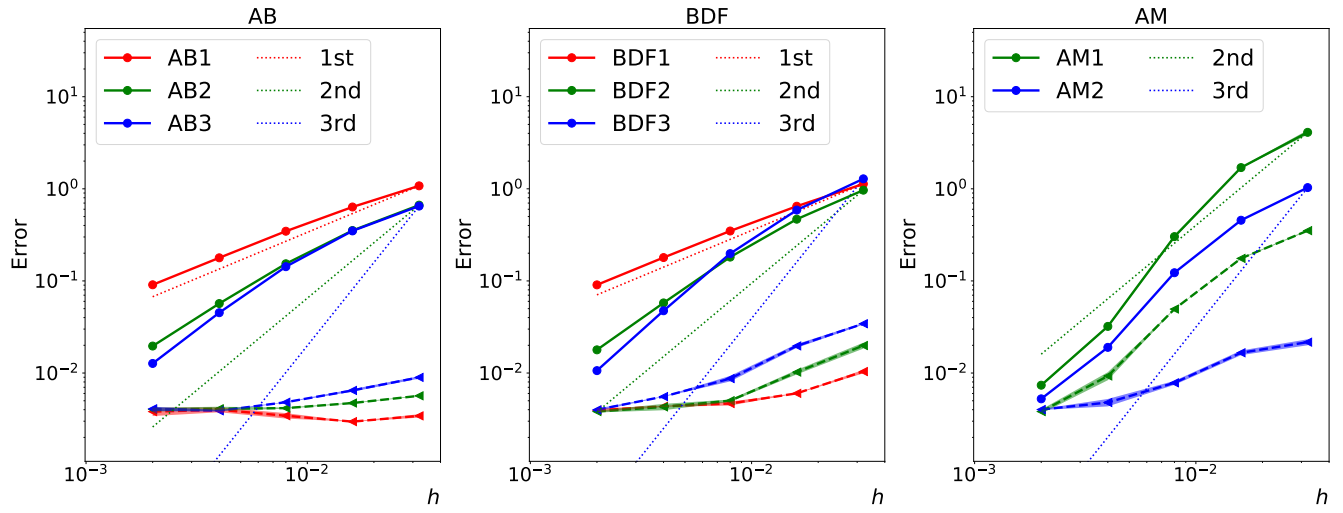


Figure 3: $\text{Error}(f_\theta, f)$ (solid curves with circle markers) and test loss (dashed curves with triangle markers) versus h for the glycolytic oscillator (26). The results are obtained by taking the mean of 5 independent experiments, and the shaded region represents one standard deviation.

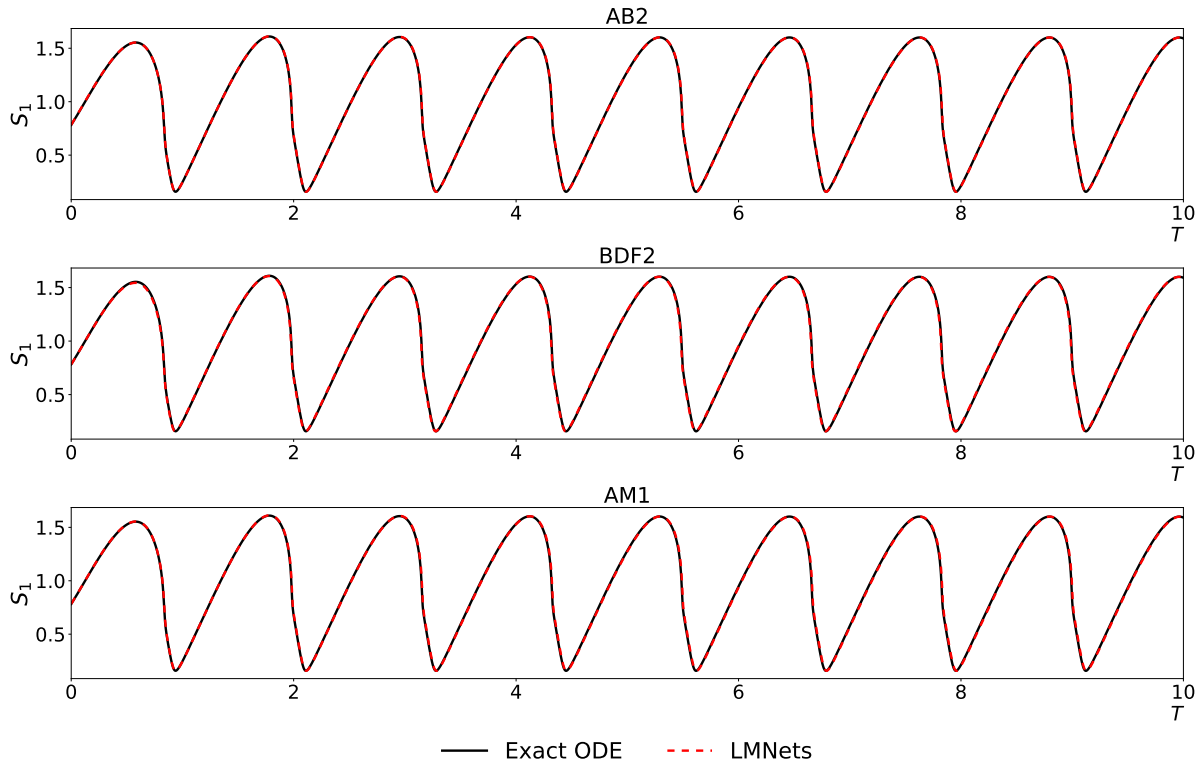


Figure 4: The first component of the trajectories of the exact system (26) and the discovered systems for the glycolytic oscillator (26).

of all schemes are lower than the theoretical ones when h is relatively large. These observations are in agreement with the numerical results in [15], which are caused by the low regularity of the glycolytic oscillator (26). Compared to the stable schemes AB, BDF, it is observed that the unstable schemes AM can also learn hidden dynamics and are more accurate when h is relatively small due to the smaller leading terms of $f_h - f$ (given in Table 3). However, when h is relatively large, due to the unstable properties when used for discovery [15], it is difficult to train and the errors would be large.

We also perform predictions for the glycolytic oscillator. We use the first trajectory in the test data as the baseline and simulate the discovered systems using the same initial condition, where the test schemes are AB($M = 2$), BDF($M = 2$), and AM($M = 1$), and the data step size is $h = 0.002$. The first components of the trajectories are depicted in Fig. 4 for comparison. It is observed that all schemes can correctly capture the form of the dynamics.

6 Summary

We provide an error analysis for the discovery of dynamics using linear multistep methods with deep learning in this paper. We show that training such a learning model returns a close approximation of the IMDE, and thereby we prove that the error between the discovered system and the target dynamical system is bounded by the sum of the LMM discretization error $\mathcal{O}(h^p)$ and the learning loss. Our conclusions (i) do not depend on auxiliary conditions; (ii) hold for any weakly stable and consistent LMM; (iii) and are able to quantify the error out of the sample locations. Moreover, numerical results support the theoretical analysis.

The analysis in this paper is restricted to the discovery of low-frequency dynamics and fine data step. For relatively large data step, this paper does not improve the existing stability analysis and error estimation [32, 15], which still remain unknown without the help of auxiliary conditions. For the discovery of dynamics with high-frequencies, we may need to design specific discretization schemes to construct loss functions, and develop corresponding error analysis. One possible direction is the filtered integrator and the modulated Fourier expansion [22].

To the best of our knowledge, general theoretical evidences and precise descriptions that justify the underlying mechanism of implicit regularization are still open research problems. As the analyticity hypotheses are closely related to implicit regularization, we would like to further investigate these hypotheses from the perspective of frequency principle/spectral bias of general neural networks in the future.

References

- [1] J. Anderson, I. Kevrekidis, and R. Rico-Martinez. A comparison of recurrent training algorithms for time series analysis and system identification. *Computers & chemical engineering*, 20:S751–S756, 1996.
- [2] G. Benettin and A. Giorgilli. On the hamiltonian interpolation of near-to-the-identity symplectic mappings with application to symplectic integration algorithms. *Journal of Statistical Physics*, 74(5):1117–1143, 1994.

- [3] T. Bertalan, F. Dietrich, I. Mezić, and I. G. Kevrekidis. On learning hamiltonian systems from data. *Chaos: An Interdisciplinary Journal of Nonlinear Science*, 29(12):121107, 2019.
- [4] J. Bongard and H. Lipson. Automated reverse engineering of nonlinear dynamical systems. *Proceedings of the National Academy of Sciences*, 104(24):9943–9948, 2007.
- [5] A. Botev, A. Jaegle, P. Wirnsberger, D. Hennes, and I. Higgins. Which priors matter? benchmarking models for learning latent dynamics. In *35th Conference on Neural Information Processing Systems (NeurIPS 2021) Track on Datasets and Benchmarks*, 2021.
- [6] S. L. Brunton, B. W. Brunton, J. L. Proctor, E. Kaiser, and J. N. Kutz. Chaos as an intermittently forced linear system. *Nature communications*, 8(1):1–9, 2017.
- [7] S. L. Brunton and J. N. Kutz. *Data-driven science and engineering: Machine learning, dynamical systems, and control*. Cambridge University Press, 2019.
- [8] S. L. Brunton, J. L. Proctor, and J. N. Kutz. Discovering governing equations from data by sparse identification of nonlinear dynamical systems. *Proceedings of the National Academy of Sciences*, 113(15):3932–3937, 2016.
- [9] R. B. Burckel. *An introduction to classical complex analysis*, volume 1. Academic Press, 1980.
- [10] Y. Cao, Z. Fang, Y. Wu, D. Zhou, and Q. Gu. Towards understanding the spectral bias of deep learning. In *Proceedings of the Thirtieth International Joint Conference on Artificial Intelligence (IJCAI 2021)*, pages 2205–2211, 2021.
- [11] T. Chen, Y. Rubanova, J. Bettencourt, and D. Duvenaud. Neural ordinary differential equations. In *32nd Conference on Neural Information Processing Systems (NeurIPS 2018)*, pages 6572–6583, 2018.
- [12] G. Cybenko. Approximation by superpositions of a sigmoidal function. *Mathematics of control, signals and systems*, 2(4):303–314, 1989.
- [13] B. C. Daniels and I. Nemenman. Efficient inference of parsimonious phenomenological models of cellular dynamics using s-systems and alternating regression. *Plos One*, 10(3), 2014.
- [14] R. Devore, B. Hanin, and G. Petrova. Neural network approximation. *Acta Numerica*, 30:327–444, 2021.
- [15] Q. Du, Y. Gu, H. Yang, and C. Zhou. The discovery of dynamics via linear multistep methods and deep learning: error estimation. *SIAM Journal on Numerical Analysis*, 60(4):2014–2045, 2022.
- [16] K. Feng. Formal power series and numerical algorithms for dynamical systems. In *Proceedings of international conference on scientific computation, Hangzhou, China, Series on Appl. Math. Singapore: World Scientific*, volume 1, pages 28–35, 1991.
- [17] K. Feng. Formal dynamical systems and numerical algorithms. *SERIES ON APPLIED MATHEMATICS*, 4:1–10, 1993.

- [18] R. González-García, R. Rico-Martínez, and I. G. Kevrekidis. Identification of distributed parameter systems: A neural net based approach. *Computers & chemical engineering*, 22:S965–S968, 1998.
- [19] S. Greydanus, M. Dzamba, and J. Yosinski. Hamiltonian neural networks. In *33rd Conference on Neural Information Processing Systems (NeurIPS 2019)*, pages 15353–15363, 2019.
- [20] E. Hairer. Backward error analysis for multistep methods. *Numerische Mathematik*, 84(2):199–232, 1999.
- [21] E. Hairer and C. Lubich. The life-span of backward error analysis for numerical integrators. *Numerische Mathematik*, 76(4):441–462, 1997.
- [22] E. Hairer and C. Lubich. Long-time energy conservation of numerical methods for oscillatory differential equations. *SIAM Journal on Numerical Analysis*, 38(2):414–441, 2001.
- [23] E. Hairer, C. Lubich, and G. Wanner. *Geometric numerical integration: structure-preserving algorithms for ordinary differential equations*, volume 31. Springer Science & Business Media, 2006.
- [24] E. Hairer and G. Wanner. *Solving ordinary differential equations I*, volume 375. Springer Berlin Heidelberg, 1996.
- [25] M. Hersch, F. Guenter, S. Calinon, and A. Billard. Dynamical system modulation for robot learning via kinesthetic demonstrations. *IEEE Transactions on Robotics*, 24(6):1463–1467, 2008.
- [26] K. Hornik, M. Stinchcombe, and H. White. Universal approximation of an unknown mapping and its derivatives using multilayer feedforward networks. *Neural Networks*, 3(5):551 – 560, 1990.
- [27] P. Hu, W. Yang, Y. Zhu, and L. Hong. Revealing hidden dynamics from time-series data by odenet. *Journal of Computational Physics*, 461:111203, 2022.
- [28] I. Huh, E. Yang, S. J. Hwang, and J. Shin. Time-reversal symmetric ODE network. In *34th Conference on Neural Information Processing Systems (NeurIPS 2020)*, 2020.
- [29] Y. Jiang, B. Neyshabur, H. Mobahi, D. Krishnan, and S. Bengio. Fantastic generalization measures and where to find them. In *8th International Conference on Learning Representations (ICLR 2020)*, 2020.
- [30] K. Kawaguchi. Deep learning without poor local minima. In *30th Conference on Neural Information Processing Systems (NIPS 2016)*, pages 586–594, 2016.
- [31] K. Kawaguchi, L. P. Kaelbling, and Y. Bengio. Generalization in deep learning. *arXiv preprint arXiv:1710.05468*, 2017.
- [32] R. T. Keller and Q. Du. Discovery of dynamics using linear multistep methods. *SIAM Journal on Numerical Analysis*, 59(1):429–455, 2021.

- [33] D. P. Kingma and J. Ba. Adam: A method for stochastic optimization. In *3rd International Conference on Learning Representations (ICLR 2015)*, 2015.
- [34] J. Kocijan, A. Girard, B. Banko, and R. Murray-Smith. Dynamic systems identification with gaussian processes. *Mathematical and Computer Modelling of Dynamical Systems*, 11(4):411–424, 2005.
- [35] J. Z. Kolter and G. Manek. Learning stable deep dynamics models. In *33rd Conference on Neural Information Processing Systems (NeurIPS 2019)*, pages 11126–11134, 2019.
- [36] J. Levinson, J. Askeland, J. Becker, J. Dolson, D. Held, S. Kammel, J. Z. Kolter, D. Langer, O. Pink, V. Pratt, et al. Towards fully autonomous driving: Systems and algorithms. In *2011 IEEE intelligent vehicles symposium (IV)*, pages 163–168. IEEE, 2011.
- [37] E. N. Lorenz. Deterministic nonperiodic flow. *Journal of atmospheric sciences*, 20(2):130–141, 1963.
- [38] J. Lu, Z. Shen, H. Yang, and S. Zhang. Deep network approximation for smooth functions. *SIAM Journal on Mathematical Analysis*, 53(5):5465–5506, 2021.
- [39] Y. Lu, S. Lin, G. Chen, and J. Pan. Modlanets: Learning generalisable dynamics via modularity and physical inductive bias. In *International Conference on Machine Learning (ICML 2022)*, volume 162, pages 14384–14397. PMLR, 2022.
- [40] T. Qin, K. Wu, and D. Xiu. Data driven governing equations approximation using deep neural networks. *Journal of Computational Physics*, 395:620–635, 2019.
- [41] N. Rahaman, A. Baratin, D. Arpit, F. Draxler, M. Lin, F. A. Hamprecht, Y. Bengio, and A. C. Courville. On the spectral bias of neural networks. In *Proceedings of the 36th International Conference on Machine Learning (ICML 2019)*, volume 97, pages 5301–5310. PMLR, 2019.
- [42] M. Raissi, P. Perdikaris, and G. E. Karniadakis. Machine learning of linear differential equations using gaussian processes. *Journal of Computational Physics*, 348:683–693, 2017.
- [43] M. Raissi, P. Perdikaris, and G. E. Karniadakis. Multistep neural networks for data-driven discovery of nonlinear dynamical systems. *arXiv preprint arXiv:1801.01236*, 2018.
- [44] S. Reich. Backward error analysis for numerical integrators. *SIAM Journal on Numerical Analysis*, 36(5):1549–1570, 1999.
- [45] R. Rico-Martinez, J. Anderson, and I. Kevrekidis. Continuous-time nonlinear signal processing: a neural network based approach for gray box identification. In *Proceedings of IEEE Workshop on Neural Networks for Signal Processing*, pages 596–605. IEEE, 1994.
- [46] R. Rico-Martinez and I. G. Kevrekidis. Continuous time modeling of nonlinear systems: A neural network-based approach. In *IEEE International Conference on Neural Networks*, pages 1522–1525. IEEE, 1993.
- [47] S. H. Rudy, S. L. Brunton, J. L. Proctor, and J. N. Kutz. Data-driven discovery of partial differential equations. *Science Advances*, 3(4):e1602614, 2017.

- [48] V. Scheidemann. *Introduction to complex analysis in several variables*. Springer, 2005.
- [49] M. Schmidt and H. Lipson. Distilling free-form natural laws from experimental data. *Science*, 324(5923):81–85, 2009.
- [50] C. Sparrow. *The Lorenz equations: bifurcations, chaos, and strange attractors*, volume 41. Springer Science & Business Media, 2012.
- [51] X. Xie, G. Zhang, and C. G. Webster. Non-Intrusive Inference Reduced Order Model for Fluids Using Deep Multistep Neural Network. *Mathematics*, 7(8):1–15, August 2019.
- [52] Z. J. Xu, Y. Zhang, and T. Luo. Overview frequency principle/spectral bias in deep learning. *arXiv preprint arXiv:2201.07395*, 2022.
- [53] Z. J. Xu, Y. Zhang, and Y. Xiao. Training behavior of deep neural network in frequency domain. In *Neural Information Processing - 26th International Conference (ICONIP)*, pages 264–274. Springer, 2019.
- [54] H. Yu, X. Tian, W. E, and Q. Li. Onsagnet: Learning stable and interpretable dynamics using a generalized onsager principle. *Physical Review Fluids*, 6(11):114402, 2021.
- [55] C. Zhang, S. Bengio, M. Hardt, B. Recht, and O. Vinyals. Understanding deep learning (still) requires rethinking generalization. *Communications of the ACM*, 64(3):107–115, feb 2021.
- [56] Z. Zhang, Y. Shin, and G. Em Karniadakis. Gfinns: Generic formalism informed neural networks for deterministic and stochastic dynamical systems. *Philosophical Transactions of the Royal Society A*, 380(2229):20210207, 2022.
- [57] Y. D. Zhong, B. Dey, and A. Chakraborty. Extending lagrangian and hamiltonian neural networks with differentiable contact models. In *35th Conference on Neural Information Processing Systems (NeurIPS 2021)*, pages 21910–21922, 2021.
- [58] A. Zhu, P. Jin, B. Zhu, and Y. Tang. On numerical integration in neural ordinary differential equations. In *Proceedings of the 39th International Conference on Machine Learning (ICML 2022)*, volume 162, pages 27527–27547. PMLR, 2022.